

Synthesis and properties of the ditelluroethers *m*- and *p*-C₆H₄(CH₂TeMe)₂ and their Te(IV) derivatives: crystal structures of PhTeI₂(CH₂)₃TeI₂Ph, *m*-C₆H₄(CH₂TeI₂Me)₂ and *p*-C₆H₄(CH₂TeI₂Me)₂

Matthew J. Hesford, Nicholas J. Hill, William Levason, Gillian Reid *

Department of Chemistry, University of Southampton, Highfield, Southampton SO17 1BJ, UK

Received 20 October 2003; accepted 8 December 2003

Abstract

The new ditelluroethers *m*-C₆H₄(CH₂TeMe)₂ and *p*-C₆H₄(CH₂TeMe)₂ have been prepared in good yield from nucleophilic reaction of *m*- or *p*-C₆H₄(CH₂Br)₂ and LiTeMe in THF solution. Reaction of the new ditelluroethers with MeI or I₂ affords the light yellow *m*- or *p*-C₆H₄(CH₂TeMe₂I)₂ or the red/orange *m*- or *p*-C₆H₄(CH₂TeI₂Me)₂, respectively in high yield. These compounds have been characterised by IR, ¹H, ¹³C{¹H} and ¹²⁵Te{¹H} NMR spectroscopy and EI mass spectrometry as appropriate. The crystal structures of the di-iodo derivatives *m*-C₆H₄(CH₂TeI₂Me)₂, *p*-C₆H₄(CH₂TeI₂Me)₂ and the related PhI₂Te(CH₂)₃TeI₂Ph (prepared from PhTe(CH₂)₃TePh and diiodine in THF solution) are described. In each compound the TeI₂ units are axial and significant intermolecular Te···I secondary contacts (≈3.6–4.1 Å) are evident, which link these covalent compounds into extended networks with each Te atom in a distorted 6-coordinate environment.

© 2004 Elsevier B.V. All rights reserved.

Keywords: Tellurium; X-ray structures; Secondary interactions

1. Introduction

We have been interested for some time in the synthesis and coordination chemistry of polydentate and macrocyclic telluroether ligands with transition metal and p-block ions [1–8]. Unlike thioether chemistry, where the ligand synthesis is not affected significantly by the inter-donor linkage, in telluroethers the choice of inter-donor linkage can play an important role in determining the course of the organotellurium reaction chemistry and thus, only a restricted range of linking units have been incorporated to-date [1]. However, the inter-donor unit can also influence considerably the metal binding properties of the ligands, hence we wish to extend the range of di- and poly-telluroether compounds to investigate these factors further. In the course of our

characterisation of new telluroethers we often prepare methiodide or diiodide Te(IV) derivatives, since these are air-stable and therefore more easily handled, e.g. the macrocyclic Te(IV) di-iodides [11]aneS₂TeI₂ (1,4-dithia-8,8-diiodo-8-telluracycloundecane) and [12]aneS₂TeI₂ (1,5-dithia-9,9-diiodo-9-telluracyclododecane) and the telluronium species [9]aneS₂TeMeI (1,4-dithia-7-methyl-7-iodo-7-telluracyclononane), [11]aneS₂TeMeI (1,4-dithia-8-methyl-8-iodo-8-telluracycloundecane) and [12]aneS₂TeMeI (1,5-dithia-9-methyl-9-iodo-9-telluracyclododecane) [7] and IMeRTe(CH₂)₃TeMeI (R = Me or Ph) [6].

Several classes of organotelluronium halide compounds are known, including species of general formula RTeX₃, R₂TeX₂ and R₃TeX and these have been reviewed [9]. In addition to their value in providing supporting spectroscopic characterisation for the telluroethers, these Te(IV) compounds are themselves often structurally very interesting, owing to the occurrence of secondary Te···X bonding interactions which can result

* Corresponding author. Tel.: +44-238-059-3609; fax: +44-238-059-3781.

E-mail address: gr@soton.ac.uk (G. Reid).

in dimeric or higher oligomeric assemblies [9,10]. We have previously examined the structure adopted by the telluronium derivative of the xylyl-linked *o*-C₆H₄(CH₂TeMe)₂ [11]. The crystal structure of *o*-C₆H₄(CH₂TeMe₂I) shows a weakly associated dimer, assembled through a series of secondary Te···I interactions to give a *pseudo*-cubane Te₄I₄ core, involving 3-coordinate (pyramidal) iodine and 6-coordinate (distorted octahedral) tellurium. The *o*-xylyl backbone units are oriented across the diagonal of two opposite faces of the cubane. The unusual motif in this species prompted us to probe the occurrence of secondary bonding interactions in other Te(IV) iodide compounds derived from related xylyl-based ditelluroethers.

In this paper we describe preparations for the new ditelluroethers *m*- and *p*-C₆H₄(CH₂TeMe)₂ which incorporate linkages likely to lead to extended networks upon coordination to metal ions. The preparation and spectroscopic characterisation of the tellurium(IV) derivatives *m*- and *p*-C₆H₄(CH₂TeMe₂I)₂ and *m*- and *p*-C₆H₄(CH₂TeI₂Me)₂ are also described. Crystal structures of the di-iodo Te(IV) species, *m*- and *p*-C₆H₄(CH₂TeI₂Me)₂ and the related PhTeI₂(CH₂)₃TeI₂Ph, are presented and the structures compared with relevant literature examples.

2. Results and discussion

The new xylyl-based ditelluroether compounds *m*- and *p*-C₆H₄(CH₂TeMe)₂ were obtained in good yield by reaction of freshly ground elemental tellurium with MeLi at 77 K in THF, which upon warming to room temperature produces MeTeLi. Addition of 0.5 mol. equivs. of *m*-C₆H₄(CH₂Br)₂ or *p*-C₆H₄(CH₂Br)₂ to this at 77 K and warming to RT affords the two new telluroethers *m*-C₆H₄(CH₂TeMe)₂ or *p*-C₆H₄(CH₂TeMe)₂ respectively as air-sensitive, yellow solids in good yield. These formulations follow from their ¹H and ¹³C{¹H} NMR spectra, with the latter showing the diagnostic δ(TeMe) at ca. -20 ppm. These compounds also show a single ¹²⁵Te{¹H} resonance, coincidentally both occur at 311 ppm. These compare with δ 264 in the related *o*-C₆H₄(CH₂TeMe)₂ [3]. The substitution patterns in the xylyl linkages of these compounds would suggest that they are less likely to chelate to metal ions than the *o*-C₆H₄(CH₂TeMe)₂.

Reaction of these compounds with excess MeI in CH₂Cl₂ solution affords the telluronium salts *m*- or *p*-C₆H₄(CH₂TeMe₂I)₂ (from microanalytical data) as light yellow powdered solids in good yield. Electrospray mass spectrometry (MeCN) shows the dicationic [*m*-/*p*-C₆H₄(CH₂TeMe₂)₂]²⁺ as the major species, with minor fragments involving loss of Me units also evident. Unlike the corresponding *o*-C₆H₄(CH₂TeMe₂I)₂ which shows reasonable solubility in CHCl₃, the *m*- and *p*-analogues are

poorly soluble in chlorocarbon solvents, hence NMR measurements were made using solutions in d⁶-dms_o. The ¹H NMR spectra show resonances consistent with conversion of Te(II) to Te(IV). The ¹³C{¹H} NMR spectra show significant high frequency shifts in δ(Me) [7.1 ppm and 6.9 ppm, respectively], and a high frequency shift in the ¹²⁵Te{¹H} NMR resonance to 531 and 537 ppm for the *m*- and *p*-derivatives, respectively (compare 526 for *o*-C₆H₄(CH₂TeMe₂I)₂) [11].

The *o*-, *m*- and *p*-C₆H₄(CH₂TeMe)₂ also react with di-iodine in THF solution to give the Te(IV) halide compounds *o*-, *m*- or *p*-C₆H₄(CH₂TeI₂Me)₂ as red/orange solids in good yield. These assignments follow from microanalytical, IR and ¹H NMR spectroscopic data. The *o*-C₆H₄(CH₂TeI₂Me)₂ decomposes appreciably over an hour or so in solution, hence ¹³C{¹H} and ¹²⁵Te{¹H} NMR data were not obtained for this species. However, ¹³C{¹H} NMR data for *m*- and *p*-C₆H₄(CH₂TeI₂Me)₂ are in accord with expectations. Most notable is the high frequency shift in δ(Me) and δ(CH₂) which accompanies the conversion from Te(II) to Te(IV). Also, δ(¹²⁵Te{¹H}) for the *m*- and *p*-C₆H₄(CH₂TeI₂Me)₂ (738 and 739 ppm) lie to higher frequency than for the Te(IV) methiodide derivatives above, consistent with other diorgano-Te(IV)-diiodide compounds, cf. PhMeTeI₂ 698 ppm [12].

In order to examine the occurrence and extent of Te···I secondary interactions, and the effect of these on the environment at tellurium, crystallographic analyses of certain of the Te(IV) derivatives were sought. Single crystals of *m*-C₆H₄(CH₂TeI₂Me)₂, *p*-C₆H₄(CH₂TeI₂Me)₂ and the related PhI₂Te(CH₂)₃TeI₂Ph were obtained as described in Section 3. The crystal structure of *m*-C₆H₄(CH₂TeI₂Me)₂ (Fig. 1, Table 1) confirms that this is an essentially covalent compound with two iodines coordinated to each Te atom in an axial arrangement (hence Te(IV) formally), with the -CH₂TeI₂Me units lying directed on opposite sides of the arene unit. The geometry at each Te is *pseudo*-trigonal bipyramidal, with the Te-based lone pair assumed to occupy the vacant equatorial vertex. The primary Te-I bonds lie in the range = 2.870(2)–2.997(2) Å, in accord with d(Te-I) in other Te(IV) iodide compounds such as [12]aneS₂TeI₂ (2.8990(9), 2.9179(9) Å) [7] and 1,1-diiodo-3,4-benzo-1-telluracyclopentane (2.928, 2.900 Å) [13]. Examination of the crystal packing in *m*-C₆H₄(CH₂TeI₂Me)₂ also shows significant longer range (secondary) Te···I interactions (Te1···I4' = 3.760(2), Te2···I2'' = 3.686 Å) between adjacent molecules which link them into an infinite array. There is a further long intermolecular Te···I contact to each Te atom (Te1-I2''' = 4.110(2), Te2-I3'''' = 4.059(2) Å). The van der Waals radii for Te and I are 2.20 and 2.15 Å, respectively [14], hence these too may be considered as weak contacts. In addition to the four primary bonds at each Te centre (2C and 2I) there are therefore two secondary

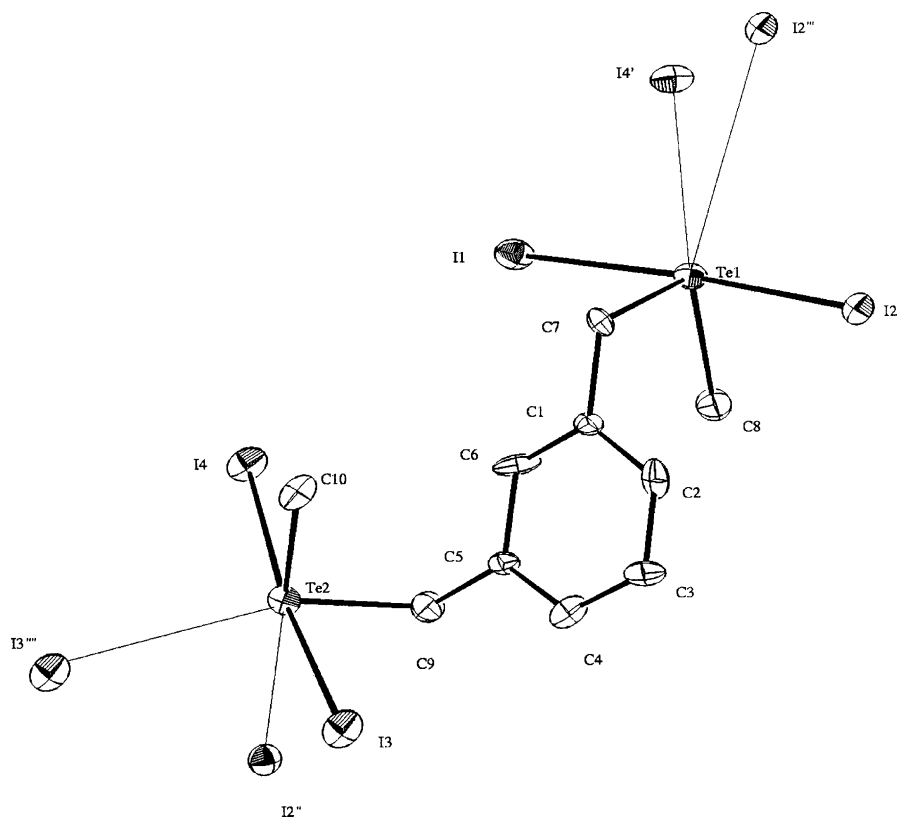


Fig. 1. View of the structure of $m\text{-C}_6\text{H}_4(\text{CH}_2\text{TeI}_2\text{Me})_2$ with numbering scheme adopted showing the coordination environment at each Te, including the secondary (intermolecular) $\text{Te}\cdots\text{I}$ contacts (symmetry operations: $' = 1 - x, y - \frac{1}{2}, -z + \frac{1}{2}$; $'' = x, 1\frac{1}{2} - y, z + \frac{1}{2}$; $''' = 1 - x, 1 - y, -z$; $'''' = -x, 1 - y, 1 - z$). Ellipsoids are drawn at 40% probability and H atoms are omitted for clarity.

Table 1
Selected bond lengths (Å) and angles (°) for $m\text{-C}_6\text{H}_4(\text{CH}_2\text{TeI}_2\text{Me})_2$

Bond lengths (Å)	
Te1–C8 = 2.12(2)	Te1–C7 = 2.20(2)
Te1–I1 = 2.892(2)	Te1–I2 = 2.938(2)
Te1–C1 = 3.10(2)	Te1–I4' = 3.760(2)
Te2–C10 = 2.08(2)	Te2–C9 = 2.18(3)
Te2–I3 = 2.870(2)	Te2–I4 = 2.997(2)
Te2–C5 = 3.11(2)	Te2–I2'' = 3.686(2)
Te1–I2''' = 4.110(2)	Te2–I3'''' = 4.059(2)
Bond angles (°)	
C8–Te1–C7 = 99.0(9)	C8–Te1–I1 = 89.4(7)
C7–Te1–I1 = 87.3(6)	C8–Te1–I2 = 90.1(7)
C7–Te1–I2 = 87.1(6)	I1–Te1–I2 = 174.20(7)
C8–Te1–I4' = 166.0(7)	C7–Te1–I4' = 72.8(6)
I1–Te1–I4' = 101.24(6)	I2–Te1–I4' = 78.41(5)
C10–Te2–C9 = 102.0(9)	C10–Te2–I3 = 90.1(7)
C9–Te2–I3 = 89.4(7)	C10–Te2–I4 = 89.7(7)
C9–Te2–I4 = 84.2(7)	I3–Te2–I4 = 173.41(8)
C10–Te2–I2'' = 170.0(7)	C9–Te2–I2'' = 74.6(6)
I3–Te2–I2'' = 99.15(6)	I4–Te2–I2'' = 80.62(5)

Symmetry operations: $' = 1 - x, y - \frac{1}{2}, -z + \frac{1}{2}$; $'' = x, 1\frac{1}{2} - y, z + \frac{1}{2}$; $''' = 1 - x, 1 - y, -z$; $'''' = -x, 1 - y, 1 - z$.

interactions, giving a distorted octahedral environment at Te.

The crystal structure of the *para*-substituted analogue, $p\text{-C}_6\text{H}_4(\text{CH}_2\text{TeI}_2\text{Me})_2$, was also determined to allow us to probe the influence that the substitution

pattern has on the gross structure. The structure of this compound is centrosymmetric, with an inversion centre at the mid-point of the arene ring (Fig. 2, Table 2), with *trans*, axial iodines bound to each Te centre. A consequence of the centre of symmetry is that the $-\text{CH}_2\text{TeI}_2\text{Me}$ units lie on opposite sides of the aromatic unit. The primary Te–I bond distances of 2.8967(8) and 2.9309(7) Å are similar to those in $m\text{-C}_6\text{H}_4(\text{CH}_2\text{TeI}_2\text{Me})_2$ above. In this species there are two significant intermolecular secondary bonding interactions to each Te, $\text{Te1}\cdots\text{I2}''' = 3.6519(8)$, $\text{Te1}\cdots\text{I1}'' = 3.7979(7)$ Å, which result in a complicated infinite array. Overall each Te1 atom is again in a very distorted octahedral environment comprising two Te–C bonds, two primary Te–I bonds and two secondary Te \cdots I bonds.

Although the secondary Te \cdots I contacts are at similar distances, the extended structures identified in these *m*- and *p*-xylyl species are quite different from the weakly associated dimer observed in $o\text{-C}_6\text{H}_4(\text{CH}_2\text{TeMe}_2\text{I})$. This is almost certainly in part due to the different architectures of the units linking the Te atoms, which prevent simple dimer formation.

The related ditelluroether $\text{PhTe}(\text{CH}_2)_3\text{TePh}$ reacts similarly with excess I_2 in THF solution to give $\text{PhTeI}_2(\text{CH}_2)_3\text{TeI}_2\text{Ph}$ as a red-black powder in moderate yield. The $^{125}\text{Te}\{^1\text{H}\}$ NMR spectrum of this product

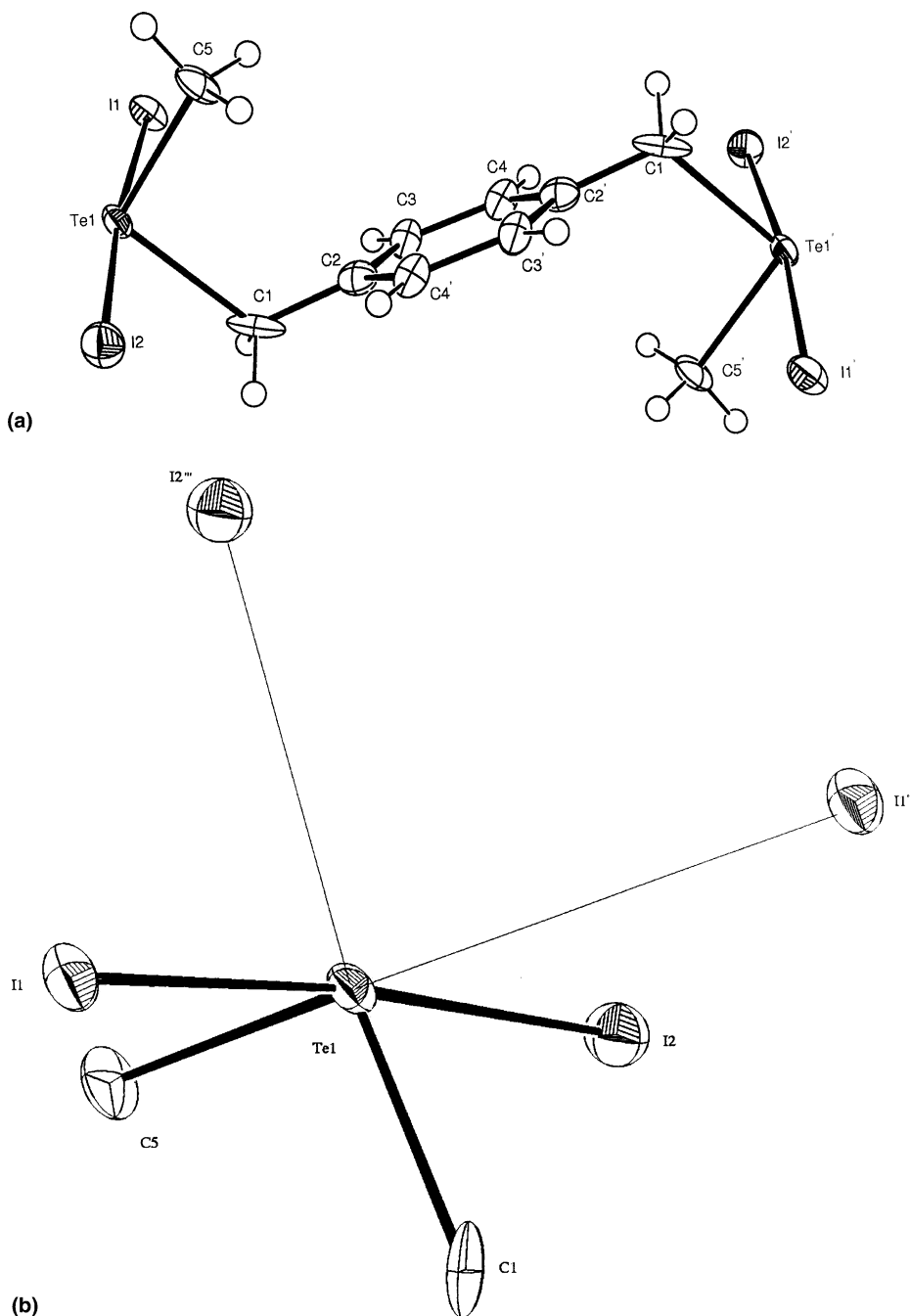


Fig. 2. (a) View of the centrosymmetric structure of $p\text{-C}_6\text{H}_4(\text{CH}_2\text{TeI}_2\text{Me})_2$ with numbering scheme adopted. Ellipsoids are drawn at 40% probability (symmetry operation: $' = 1 - x, -y, 1 - z$); (b) diagram showing the coordination environment at Te1, including the secondary (intermolecular) $\text{Te}\cdots\text{I}$ contacts (symmetry operations: $'' = 2 - x, -y, 2 - z$; $''' = x, \frac{1}{2} - y, z + \frac{1}{2}$).

shows a singlet at 651 ppm, once again significantly to high frequency of the parent telluroether (466 ppm).

The crystal structure of $\text{PhTeI}_2(\text{CH}_2)_3\text{TeI}_2\text{Ph}$ (Fig. 3, Table 3) adopts crystallographic 2-fold symmetry, with C1, the central carbon in the trimethylene linkage, occupying a 2-fold symmetry site ($0, y, \frac{3}{4}$). A similar sawhorse geometry is observed at tellurium, like in the structures above, with the iodines axial and the Te-bonded C atoms equatorial. The primary Te–I bonds lie

in the range 2.883(4)–2.938(3) Å, in accord with both *m*- and *p*- $\text{C}_6\text{H}_4(\text{CH}_2\text{TeI}_2\text{Me})_2$ above. Closer inspection of the packing of the $\text{PhTeI}_2(\text{CH}_2)_3\text{TeI}_2\text{Ph}$ units again reveals an extended network formed through secondary $\text{Te1}\cdots\text{I1}''$ interactions of 3.702(4) Å, giving weakly bound chains with the linear I–Te–I units in adjacent molecules aligned parallel and Te_2I_2 rhomboid units. Further, weaker $\text{Te1}\cdots\text{I}'''$ contacts (4.0712(6) Å) between a Te atom within each Te_2I_2 rhomboid and an I

Table 2
Selected bond lengths (Å) and angles (°) for $p\text{-C}_6\text{H}_4(\text{CH}_2\text{TeI}_2\text{Me})_2$

Bond lengths (Å)	
C1–Te1	2.241(10)
C5–Te1	2.137(8)
Te1–I1	2.8967(8)
Te1–I2	2.9309(7)
Te1–I2'''	3.6519(8)
Te1–I1''	3.7979(7)
Bond angles (°)	
C5–Te1–C1	100.7(3)
C5–Te1–I1	87.8(3)
C1–Te1–I1	89.0(2)
C5–Te1–I2	88.1(3)
C1–Te1–I2	88.1(2)
I1–Te1–I2	174.48(2)
C5–Te1–I2'''	85.3(3)
C1–Te1–I2'''	173.6(2)
I1–Te1–I2'''	93.38(2)
I2–Te1–I2'''	89.914(19)
C5–Te1–I1''	162.7(3)
C1–Te1–I1''	84.0(2)
I1–Te1–I1''	109.138(18)
I2–Te1–I1''	75.272(18)

Symmetry operations: ' = $2 - x, -y, 2 - z$; '' = $x, \frac{1}{2} - y, z + \frac{1}{2}$.

atom diagonally opposite give rise to a 'cradle-like' motif comprised of three Te_2I_2 units. One face of the cradle is shared between two units, giving an alternating 'up-down' chain arrangement, with the trimethylene linkage between the Te atoms straddling diagonally across the top of each cradle. Overall, the environment at each Te centre is *pseudo*-six coordinate, although the bond angles are severely distorted from regular octahedral.

A number of Te(IV) di-iodide compounds derived from monotelluroethers have been examined crystallographically, e.g. Me_2TeI_2 . The environment at Te in the α -form is similar to the compounds described in this work, and involves two axial iodines (2.885(3) and 2.965(3) Å), two *cis* Me groups and two weak, intermolecular $\text{Te} \cdots \text{I}$ contacts (3.659(3), 3.919(3) Å), giving an extended array [15]. These distances compare well with those reported here. The β -form subsequently turned out to be the ionic species $[\text{TeMe}_3][\text{TeMeI}_4]$ [16]. The structure of $(\text{CH}_2\{p\text{-(OMe)-C}_6\text{H}_4\text{TeI}_2\})_2$ has been described by Singh and co-workers and involves long intermolecular $\text{Te} \cdots \text{I}$ contacts of 3.735(1)–3.879(1) Å [17].

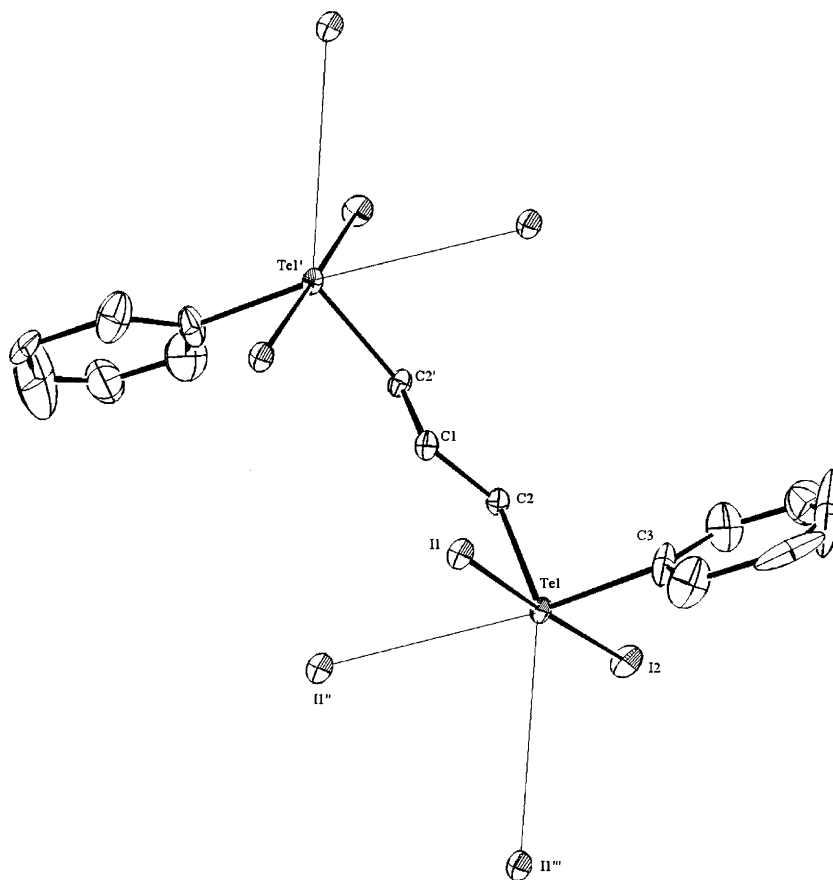


Fig. 3. View of the structure of $\text{PhTeI}_2(\text{CH}_2)_3\text{TeI}_2\text{Ph}$, with numbering scheme adopted, showing the environment at the Te centres and including intermolecular secondary interactions. Ellipsoids are drawn at 40% probability and H atoms are omitted for clarity (symmetry operations: ' = $-x, y, 1\frac{1}{2} - z$; '' = $-x, 2 - y, 1 - z$; ''' = $x, 2 - y, \frac{1}{2} + z$).

Table 3
Selected bond lengths (Å) and angles (°) for PhTeI₂(CH₂)₃TeI₂Ph

Bond lengths (Å)	
I1–Te1	2.9377(6)
I1''–Te1	3.7020(6)
I2–Te1	2.8835(6)
I1'''–Te1	4.0712(6)
Te1–C3	2.082(14)
Te1–C2	2.155(6)
Te1–C3B	2.187(17)
Bond angles (°)	
C3–Te1–C2	105.7(5)
C2–Te1–C3B	94.5(5)
C3–Te1–I2	91.5(4)
C2–Te1–I2	84.79(17)
C3B–Te1–I2	88.7(4)
C3–Te1–I1	86.5(4)
C2–Te1–I1	95.23(17)
C3B–Te1–I1	89.2(4)
I2–Te1–I1	177.93(2)
C3–Te1–I1''	175.9(4)
C2–Te1–I1''	75.04(17)
C3B–Te1–I1''	169.2(5)
I2–Te1–I1''	92.576(16)
I1–Te1–I1''	89.426(15)

Symmetry operations: '' = $-x, 2 - y, 1 - z$; ''' = $x, 2 - y, \frac{1}{2} + z$.

These results show that xylyl units involving different substitution patterns can be introduced readily as linking units in ditelluroethers. The crystallographic studies reveal interesting extended structures for the di-iodo Te(IV) complexes with significant secondary Te···I bonding interactions linking the monomer units and demonstrate that the xylyl substitution pattern, and more generally the nature of the inter-donor linking unit in these compounds also plays a significant role in determining the nature of these secondary interactions and hence the extended structures adopted.

3. Experimental

Infrared spectra were recorded as CsI discs using a Perkin–Elmer 983G spectrometer over the range 4000–200 cm⁻¹. Mass spectra were run by electron impact on a VG-70-SE Normal geometry double focusing spectrometer or by positive ion electrospray (MeCN solution) using a VG Biotech platform. ¹H NMR spectra were recorded using a Bruker AM300 spectrometer. ¹³C{¹H} and ¹²⁵Te{¹H} NMR spectra were recorded using a Bruker DPX400 spectrometer operating at 100.6 or 126.3 MHz, respectively and are referenced to TMS and external neat Me₂Te, respectively. Microanalyses were undertaken by the University of Strathclyde microanalytical service.

Solvents were dried prior to use and all preparations were undertaken using standard Schlenk techniques under a N₂ atmosphere. The ligands *o*-C₆H₄(CH₂TeMe)₂

and PhTe(CH₂)₃TePh were prepared as described previously [3,5].

3.1. Preparations

m-C₆H₄(CH₂TeMe)₂: Freshly ground tellurium powder (1.59 g, 12.5 mmol) was frozen (77 K) in THF (70 cm³) and MeLi (12.5 mmol) added. The mixture was allowed to warm to room temperature and stirred for 30 min to form a clear yellow solution of MeTeLi. The mixture was then refrozen (77 K) and a solution of *m*-C₆H₄(CH₂Br)₂ (1.65 g, 6.25 mmol) in dry THF (30 cm³) added. The mixture was then allowed to warm to room temperature and stirred for 20 h, before hydrolysing (ca. 50 cm³ with degassed water) and extracting with CH₂Cl₂ (2 × 50 cm³). The combined organic extracts were dried (MgSO₄), filtered and the solvent removed to give a light yellow solid. Yield 1.69 g, 69%. Melting point 64 °C. EIMS: found 390 (*m*-C₆H₄(CH₂TeMe)₂). ¹H NMR (CDCl₃): δ 7.0–7.2 (m, 4H, *m*-C₆H₄), 4.0 (s, 4H, CH₂), 1.95 (s, 6H, Me) ppm. ¹³C{¹H} NMR (CDCl₃): δ 141.4 (*ipso*-C, *m*-C₆H₄), 128.8 (1C, *m*-C₆H₄), 128.6 (1C, *m*-C₆H₄), 126.4 (2C, *m*-C₆H₄), 5.7 (CH₂Te), –20.1 (TeMe) ppm. ¹²⁵Te{¹H} NMR (CDCl₃): δ 311 ppm. IR (CsI disk): 3060w, 2920w, 1592w, 1584w, 1481m, 1435m, 1414m, 1263w, 1260m, 1246w, 1214m, 1150m, 1142m, 1116m, 1068m, 927w, 900w, 847m, 830m, 797m, 699m, 536m, 525w, 427w, 392w, 383w, 275w, 246w, 221w cm⁻¹.

p-C₆H₄(CH₂TeMe)₂: Method and work-up as above, using freshly ground tellurium powder (1.59 g, 12.5 mmol), MeLi (12.5 mmol) and *p*-C₆H₄(CH₂Br)₂ (1.65 g, 6.25 mmol) to give a yellow solid. Yield 1.98 g, 82%. Melting point 85 °C. EIMS: found 390 (*p*-C₆H₄(CH₂TeMe)₂). ¹H NMR (CDCl₃): δ 7.05 (s, 4H, *p*-C₆H₄), 3.9 (s, 4H, CH₂), 1.75 (s, 6H, Me) ppm. ¹³C{¹H} NMR (CDCl₃): δ 138.8 (*ipso*-C, *p*-C₆H₄), 129.0 (*p*-C₆H₄), 5.3 (CH₂Te), –20.1 (TeMe) ppm. ¹²⁵Te{¹H} NMR (CDCl₃): δ 311 ppm. IR (CsI disk): 3050w, 2925w, 2853w, 1600w, 1502m, 1457w, 1419m, 1364m, 1261m, 1214m, 1104m, 1018m, 861w, 830m, 614w, 586m, 523w, 462w, 315w, 246w, 222w cm⁻¹.

m-C₆H₄(CH₂TeMe₂I)₂: MeI (ca. 1 cm³, excess) was added to a solution of *m*-C₆H₄(CH₂TeMe)₂ (0.12 g, 0.31 mmol) in CH₂Cl₂ (50 cm³) and the mixture stirred at room temperature for 2 h. The resulting cloudy yellow solution was concentrated (ca. 25 cm³) and Et₂O (ca. 20 cm³) added. The resultant precipitate was filtered off and washed with Et₂O to give a pale yellow powdered solid. Yield 0.150 g, 72%. Required for C₁₂H₂₀I₂Te₂ · 1/2Et₂O: C, 23.7; H, 3.5%. Found: C, 24.5; H, 3.5%. Electrospray MS (MeCN): found 547 ([*m*-C₆H₄(CH₂TeMe₂)₂I]⁺), 210 ([*m*-C₆H₄(CH₂TeMe₂)₂]²⁺). ¹H NMR (d⁶-dmsO): δ 7.0–7.5 (m, 4H, *m*-C₆H₄), 4.1 (s, 4H, CH₂), 1.9 (s, 12H, Me) ppm. ¹³C{¹H} NMR (d⁶-dmsO): δ 134.7 (*ipso*-C, *m*-C₆H₄), 131.8 (1C, *m*-C₆H₄), 131.6 (1C, *m*-C₆H₄), 129.7

(2C, *m*-C₆H₄), 29.1 (CH₂Te), 7.1 (TeMe) ppm. ¹²⁵Te{¹H} NMR (d⁶-dmsO): δ 531 ppm. IR (CsI disk): 3014w, 2977w, 2922w, 2861w, 1600w, 1584w, 1483m, 1441m, 1414m, 1360m, 1227m, 1155m, 1119m, 1075w, 934w, 893w, 856m, 803m, 741w, 708m, 617w, 541m, 431w, 340w, 244w, 222w cm⁻¹.

p-C₆H₄(CH₂TeMe₂)₂: MeI (ca. 1 cm³, excess) was added to a solution of *p*-C₆H₄(CH₂TeMe)₂ (0.12 g, 0.31 mmol) in CH₂Cl₂ (50 cm³) and the mixture stirred at room temperature for 2 h. The resultant precipitate was filtered off and washed with Et₂O to give a pale yellow powdered solid. Yield 0.150 g, 72%. Required for C₁₂H₂₀I₂Te₂: C, 21.4; H, 3.0%. Found: C, 22.0; H, 3.2%. Electro-spray MS (MeCN): found 405 ([*p*-C₆H₄(CH₂TeMe)(CH₂TeMe₂)⁺], 210 ([*p*-C₆H₄(CH₂TeMe₂)₂²⁺]). ¹H NMR (d⁶-dmsO): δ 7.3 (s, 4H, *p*-C₆H₄), 4.05 (s, 4H, CH₂), 1.8 (s, 12H, Me) ppm. ¹³C{¹H} NMR (d⁶-dmsO): δ 133.4 (*ipso*-C, *p*-C₆H₄), 130.9 (*p*-C₆H₄), 28.2 (CH₂Te), 6.9 (TeMe) ppm. ¹²⁵Te{¹H} NMR (d⁶-dmsO): δ 537 ppm. IR (CsI disk): 3017w, 2923w, 2858w, 1600w, 1506w, 1418m, 1358m, 1263w, 1227m, 1203w, 1128m, 1101m, 1018sh, 994m, 890w, 835m, 732w, 614w, 586m, 533w, 417w, 312w, 224w cm⁻¹.

o-C₆H₄(CH₂TeI₂Me)₂: To a solution of *o*-C₆H₄(CH₂TeMe)₂ (0.10 g, 0.26 mmol) in dry THF (30 cm³) was added a solution of I₂ (0.13 g, 0.51 mmol) in dry THF (10 cm³) and the solution stirred in a foil-wrapped vessel at room temperature for 2 h. The solution volume was reduced (ca. 5 cm³) and Et₂O (ca. 10 cm³) added to form a precipitate that was filtered off, washed with Et₂O and dried in vacuo to give a red/orange solid. Yield 0.067 g, 30%. Required for C₁₀H₁₄I₄Te₂: C, 13.4; H, 1.6%. Found: C, 13.8; H, 1.5%. ¹H NMR (d⁶-dmsO): δ 7.2–7.4 (m, 4H, *o*-C₆H₄), 4.30 (s, 4H, CH₂), 2.95 (s, 6H, Me) ppm. IR (CsI disk): 3020w, 2959w, 2925w, 2857w, 1595w, 1484m, 1446m, 1396w, 1359m, 1261w, 1220m, 1197w, 1128m, 1101sh, 1054m, 952w, 860w, 834sh,

797w, 761m, 615w, 555m, 523w, 325w, 300w, 247w, 223w cm⁻¹.

m-C₆H₄(CH₂TeI₂Me)₂: Method as above using *m*-C₆H₄(CH₂TeMe)₂ (0.10 g, 0.26 mmol) and I₂ (0.13 g, 0.51 mmol). Red/orange solid. Yield 0.109 g, 47%. Required for C₁₀H₁₄I₄Te₂ · 1/2Et₂O: C, 15.4; H, 2.0%. Found: C, 15.6; H, 1.4%. ¹H NMR (d⁶-dmsO): δ 7.15–7.65 (m, 4H, *m*-C₆H₄), 4.6 (s, 4H, CH₂), 2.4 (s, 6H, Me) ppm. ¹³C{¹H} NMR (CDCl₃): δ 133.2, 130.5, 130.3 (2C), 128.1 (*m*-C₆H₄), 41.3 (CH₂Te), 10.8 (TeMe) ppm. ¹²⁵Te{¹H} NMR (CDCl₃): δ 738 ppm. IR (CsI disk): 3017w, 2943w, 2858w, 1582w, 1482m, 1436w, 1406m, 1253w, 1213w, 1161m, 1150m, 1117w, 1100w, 1073m, 997w, 940w, 849m, 819w, 805m, 794m, 703m, 558w, 538sh, 531m, 394w, 348w, 324w, 300w, 224w cm⁻¹.

p-C₆H₄(CH₂TeI₂Me)₂: Method as above using *p*-C₆H₄(CH₂TeMe)₂ (0.10 g, 0.26 mmol) and I₂ (0.13 g, 0.51 mmol). Red/orange solid. Yield 0.092 g, 40%. Required for C₁₀H₁₄I₄Te₂: C, 13.4; H, 1.6%. Found: C, 13.9; H, 1.8%. ¹H NMR (d⁶-dmsO): δ 7.5 (s, 4H, *p*-C₆H₄), 4.65 (s, 4H, CH₂), 2.35 (s, 6H, Me) ppm. ¹³C{¹H} NMR (CDCl₃): δ 133.6 (*ipso*-C, *p*-C₆H₄), 129.4 (*p*-C₆H₄), 41.4 (CH₂Te), 20.9 (TeMe) ppm. ¹²⁵Te{¹H} NMR (CDCl₃): δ 739 ppm. IR (CsI disk): 3020w, 2940w, 2863w, 1540w, 1501w, 1420m, 1396sh, 1358m, 1262w, 1216w, 1138m, 1107m, 1081m, 1020w, 995m, 829m, 792w, 759w, 626w, 573m, 434w, 415w, 312w, 247w, 222w cm⁻¹.

PhTeI₂(CH₂)₃TeI₂Ph: To an anhydrous THF solution (10 cm³) of PhTe(CH₂)₃TeMe (0.11 g, 0.12 mmol) was added a THF solution (5 cm³) of I₂ (0.2 g). The red-black solution was stirred at room temperature for 2 h and the solvent was removed in vacuum to leave a dark red/orange powder, which was washed with hexane and dried in vacuo. Yield 46%. Required for C₁₅H₁₆I₄Te₂: C, 18.8; H, 1.7%. Found: C, 18.5; H, 1.5%. ¹²⁵Te{¹H} NMR (CDCl₃): δ 651.

Table 4
Crystallographic parameters

Complex	<i>m</i> -C ₆ H ₄ (CH ₂ TeI ₂ Me) ₂	<i>p</i> -C ₆ H ₄ (CH ₂ TeI ₂ Me) ₂	PhTeI ₂ (CH ₂) ₃ TeI ₂ Me
Formula	C ₁₀ H ₁₄ I ₄ Te ₂	C ₁₀ H ₁₄ I ₄ Te ₂	C ₁₅ H ₁₆ I ₄ Te ₂
M	897.01	897.01	959.11
Crystal system	Monoclinic	Monoclinic	Orthorhombic
Space group	<i>P</i> 2 ₁ / <i>c</i> (#14)	<i>P</i> 2 ₁ / <i>c</i> (#14)	<i>Pb</i> cn (#60)
<i>a</i> (Å)	10.018(2)	10.8286(7)	23.6450(2)
<i>b</i> (Å)	9.2154(18)	9.2821(3)	9.0897(2)
<i>c</i> (Å)	20.264(4)	9.4672(6)	10.1816(3)
β (°)	98.30(3)	104.816(2)	90
<i>U</i> (Å ³)	1851.2(6)	919.93(9)	2188.29(5)
<i>Z</i>	4	2	4
μ (Mo Kα)/cm ⁻¹	98.02	98.62	83.03
Unique reflections	4146	2089	2496
No. of parameters	145	74	90
<i>R</i> ₁ [<i>I</i> ₀ > 2σ(<i>I</i> ₀)]	0.0786	0.0521	0.0390
<i>wR</i> ₂ [<i>I</i> ₀ > 2σ(<i>I</i> ₀)]	0.1857	0.1283	0.0978

$$R_1 = \sum ||F_o| - |F_c|| / \sum |F_o|, wR_2 = \left[\frac{\sum_w (F_o^2 - F_c^2)^2}{\sum w F_o^4} \right]^{1/2}.$$

3.2. X-ray crystallography

Details of the crystallographic data collection and refinement parameters are given in Table 4. Orange plate crystals of *m*-C₆H₄(CH₂TeI₂Me)₂, *p*-C₆H₄(CH₂TeI₂Me)₂ and PhTeI₂(CH₂)₃TeI₂Ph were grown by slow evaporation from a solution of the appropriate compound in THF. Data collection used a Nonius Kappa CCD diffractometer (*T* = 120 K) and with graphite-monochromated Mo K_α X-radiation ($\lambda = 0.71073$ Å). Structure solution and refinement were routine [18,19], except for PhTeI₂(CH₂)₃TeI₂Ph, which showed substantial disorder of the phenyl rings. This was modelled reasonably successfully to give two almost perpendicular orientations each with 50% occupancy. Selected bond lengths and angles are given in Tables 1–3.

4. Supplementary material

Crystallographic data for the structural analyses have been deposited with the Cambridge Crystallographic Data Centre, CCDC nos. 221911–221913. Copies of this information may be obtained free of charge from The Director, CCDC, 12 Union Road, Cambridge CB2 1EZ, UK (Fax: +44-1223-336033; email: deposit@ccdc.cam.ac.uk or [www:http://www.ccdc.cam.ac.uk](http://www.ccdc.cam.ac.uk)).

Acknowledgements

We thank the EPSRC for support.

References

- [1] E.G. Hope, W. Levason, *Coord. Chem. Rev.* 122 (1993) 109; W. Levason, S.D. Orchard, G. Reid, *Coord. Chem. Rev.* 225 (2002) 159.
- [2] W. Levason, G. Reid, *J. Chem. Soc., Dalton Trans.* (2001) 2953.
- [3] W. Levason, B. Patel, G. Reid, A.J. Ward, *J. Organomet. Chem.* 619 (2001) 218.
- [4] E.G. Hope, T. Kemmitt, W. Levason, *Organometallics* 7 (1988) 78.
- [5] T. Kemmitt, W. Levason, *Organometallics* 8 (1989) 1303.
- [6] A.J. Barton, W. Levason, G. Reid, A.J. Ward, *Organometallics* 20 (2001) 3644.
- [7] W. Levason, S.D. Orchard, G. Reid, *Chem. Commun.* (2001) 427; M.J. Hesford, W. Levason, M.L. Matthews, S.D. Orchard, G. Reid, *Dalton Trans.* (2003) 2434.
- [8] M.J. Hesford, W. Levason, M.L. Matthews, G. Reid, *Dalton Trans.* (2003) 2852.
- [9] I. Hargittai, B. Rozsondai, in: S. Patai, Z. Rappoport (Eds.), *The Chemistry of Organic Selenium and Tellurium Compounds*, vol. 1, Wiley, New York, 1986 (Chapter 3).
- [10] N.W. Alcock, *Adv. Inorg. Chem Radiochem.* 122 (1972) 1.
- [11] N.J. Hill, W. Levason, G. Reid, A.J. Ward, *J. Organomet. Chem.* 642 (2002) 186.
- [12] W. McFarlane, F.J. Berry, B.C. Smith, *J. Organomet. Chem.* 113 (1973) 193.
- [13] C. Knobler, R.F. Ziolo, *J. Organomet. Chem.* 178 (1979) 423.
- [14] J. Emsley, *The Elements*, third ed., Oxford University Press, Oxford, 1998.
- [15] L.Y.Y. Chan, F.W.B. Einstein, *J. Chem. Soc., Dalton Trans.* (1972) 316.
- [16] F. Einstein, J. Trotter, C. Williston, *J. Chem. Soc. (A)* (1967) 2018.
- [17] A.K. Singh, M. Kadarkaraisamy, J.E. Drake, R.J. Butcher, *Inorg. Chim. Acta* 304 (2000) 45.
- [18] G.M. Sheldrick, *SHELXS-97*, program for crystal structure solution, University of Göttingen, 1997.
- [19] G.M. Sheldrick, *SHELXL-97*, program for crystal structure refinement, University of Göttingen, 1997.